Carpathian Journal of Earth and Environmental Sciences, February 2026, Vol. 21, No. 1, p. 35 – 48; DOI:10.26471/cjees/2026/021/350

ASSESSMENT OF SAND ENCROACHMENT IN ARID REGIONS: A CASE STUDY OF EL HAJEB MUNICIPALITY, BISKRA PROVINCE, SOUTHEASTERN SAHARA, ALGERIA

Sofiane BENSEFIA[1*], Djouheina BOUKEHLIFI KOUIDER[2] & Houria ATHMANI[3]

[1]Department of Agriculture sciences, Faculty of Life and Natural Sciences and of Earth and Universe Sciences, Health and Environment Laboratory, Mohmed El-Bachir El-Ibrahimi University, Bordj Bou Arreridj, El-Anasser, Algeria; Sofiane.bensefia@univ-bba.dz

[2]LARYSS laboratory, University Mohamed Khider, Biskra, Algeria; bk.jouhina@univ-biskra.dz

[3]Department, Faculty, Institution, Address; LARYSS laboratory, University Mohamed Khider, Biskra, Algeria

**Corresponding author: Sofiane.bensefia@univ-bba.dz*

Abstract: This study examines sand encroachment in El Hajeb, Algeria, from 2000 to 2023—a region highly vulnerable to desertification. A multi-source remote sensing framework was used, combining optical and radar satellite data (Landsat, MODIS, Sentinel-1 SAR) with spectral indices (NDVI, MSAVI, BSI, NDESI) to monitor dune dynamics, vegetation health, and sand distribution. Pre-processing steps included atmospheric correction, cloud masking, and normalization. Advanced geospatial analysis and supervised classification were conducted using machine-learning algorithms—Random Forest (RF) and Support Vector Machine (SVM)—, which improved classification accuracy and land, cover discrimination. Results show an 11.90% reduction in stabilized dunes and a 6.05% increase in sparse sand areas. These shifts are linked to vegetation exploitation, soil moisture status, and intensified aeolian activity driven by prolonged droughts and prevailing winds. Sentinel-1 SAR data contributed to understanding surface roughness and moisture variability, reinforcing the analysis. Spatial maps revealed high-risk zones along the periphery of vegetated areas. To combat land degradation, the study recommends windbreaks, sand fences, and afforestation efforts. Overall, the research highlights the value of integrating remote sensing and machine learning for environmental monitoring and supports the development of adaptive land management strategies to enhance resilience in arid landscapes.

Keywords: sand encroachment, desertification, remote sensing, machine learning, sustainability and management, Elhajdeb region

1. INTRODUCTION

The interaction between wind, water, and land plays a central role in shaping contemporary geomorphology, particularly in arid and semi-arid regions (Nash & McLaren, 2003). In these areas, increasing anthropogenic pressures—such as overgrazing, deforestation, and poor land management—have accelerated the desertification process (Manière & Chamignon, 1986). Continuous monitoring is therefore crucial, especially in regions vulnerable to sand encroachment driven by climate change and unsustainable human activities (Mihi et al., 2019).

In Algeria, early foundational studies by Kasbadji Merzouk (1999) and McKee (1979) provided important wind and dune movement mapping, laying the groundwork for contemporary desertification research. Today, approximately 20 million hectares are at risk of wind erosion, with 5 million hectares already severely degraded (Bensaïd, 2006). The Saharan Atlas Mountains, forming a natural barrier at the Sahara's edge, are key zones for understanding wind patterns and sand accumulation (Benazzouz, 1994).

Historical records further show that northwest Biskra, particularly around El Hajeb, has experienced periodic sand and gypsum dust flows dating back to

the Upper Pleistocene and Holocene periods (Ballais et al., 1979).

The Hodna Basin and surrounding areas contribute significantly to sand transport southward and into dune formation systems such as the Grand Erg Oriental.

Several regional studies have focused on high-risk zones such as Tebessa Province (Logistic Regression), the Hodna Basin and Boussaada Sub-Basin (MEDALUS model), and the High Plateaus (phytoecological analysis), confirming that vegetation loss, soil texture, and poor land management are key desertification drivers (e.g., Nemamcha, Hodna, and In-Salah studies).

Remote sensing has become indispensable for large-scale environmental monitoring, providing valuable data for tracking drought patterns and sand movement (Wu & Wilhite, 2004). Drought impacts ecosystems, agriculture, and water security, and indicators like NDVI, LST, and soil moisture—derived from satellite imagery—allow for precise detection of stress conditions (Jain & Singh, 2003).

Long-term satellite observations, as demonstrated in studies like Graw et al. (2019) and Cullen (2023), aid in early warning and resilience planning. Projects such as EvIDENz further emphasize integrating socio-economic data to assess vulnerability comprehensively.

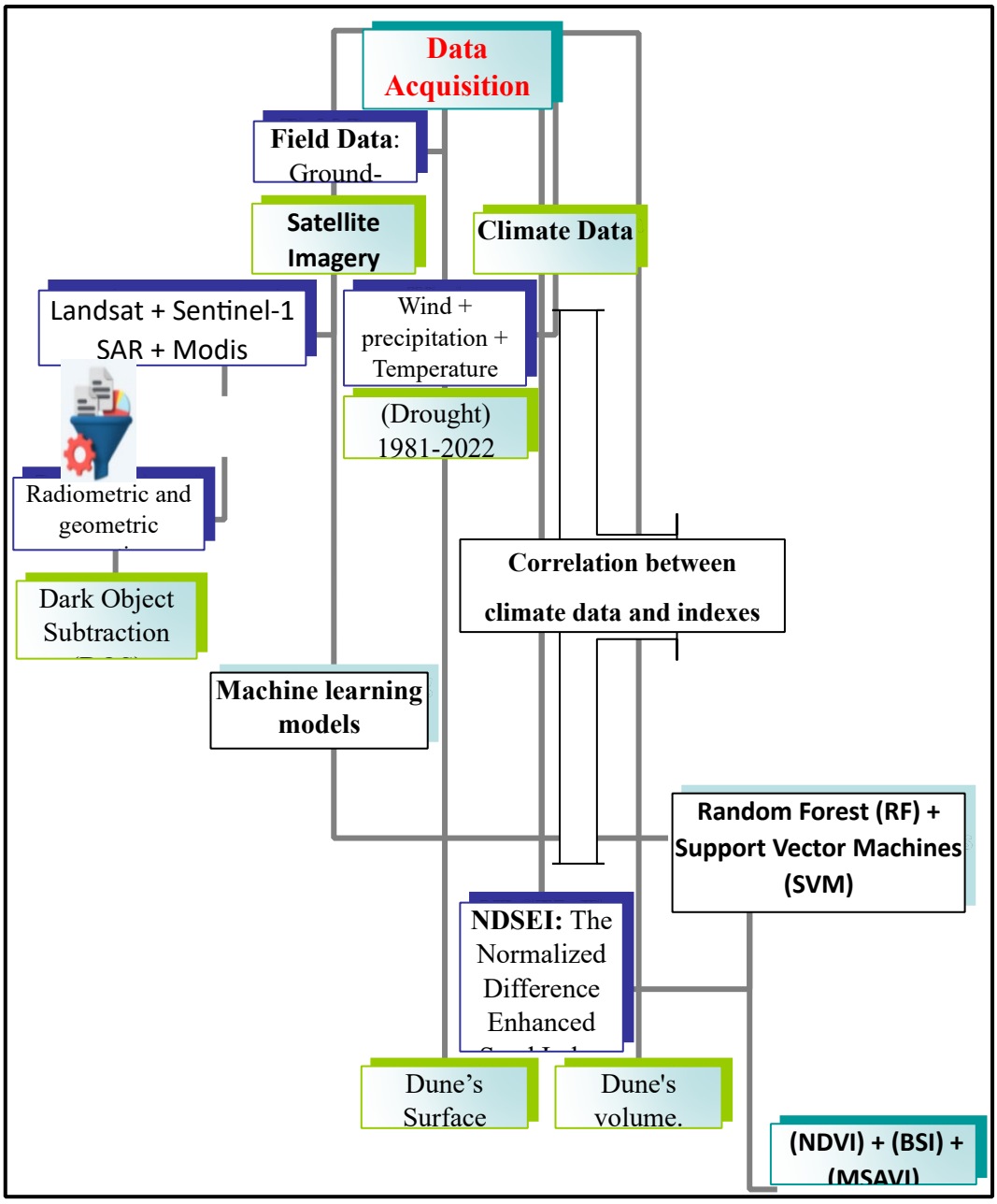

Figure 1. Methodology adopted

In Algeria, remote sensing and GIS have been widely used for LULC change detection, sand encroachment tracking, and forest degradation (e.g., Boulghobra et al., 2014). Recent research in areas like Djelfa, Soummam Valley, and Blida has employed Landsat, Sentinel, and machine learning techniques (SVM, Markov Chains) to model land degradation trends and forecast risk zones.

This study focuses on El Hajeb (Biskra), a critical transitional zone for aeolian sand movement towards northern Algeria. Over the past two decades, this region has faced intensified sand encroachment, exacerbated by vegetation decline, drought, and high wind velocity. By leveraging multi-temporal satellite datasets (Landsat, MODIS, and Sentinel-2), climate records, and field data, we apply advanced machine learning models—Random Forest (RF) and Support Vector Machines (SVM)—to classify and analyze spatial and temporal patterns of sand encroachment, vegetation loss, and bare soil expansion (Figure 1).

Advanced spectral indices such as NDVI, MSAVI, BSI, and NDESI are employed alongside SAR data to enhance surface characterization (Figure 1). Wind erosion modeling and temporal analyses allow the identification of active dune fronts and high-risk corridors. A specific focus is placed on National Road No. 46, a vital transport axis connecting Biskra to Algiers, which has been recurrently threatened by advancing dunes.

To mitigate degradation, this research simulates the impact of interventions such as windbreaks, sand fences, and afforestation, integrating remote sensing outputs with spatial models. The combination of climate data, satellite imagery, and machine learning provides a robust and scalable framework for environmental monitoring and resilience planning in Algeria's arid zones.

2. MATERIALS AND METHODS

2.1. Study Area

The municipality of El Hajeb is situated to the west of Biskra Town. It is bordered to the north by Loutaya, to the south by Oumache, to the west by Bouchekroun, and to the east by Biskra. This positioning makes it a key link between the eastern and western parts of the Wilaya. National Road No. 46, a crucial transport artery connecting the Wilaya to the capital, Algiers, traverses the area. El Hajeb includes the secondary communities of Zaachata Ben Boulaid, Bordj El Nos, and Ain El Karma, and covers an area of 208.10 km². (Figure 2).

The region lies between two opposing views between two significant mountain ranges: the Saharan Atlas and the Sahara Desert. Among the topographical features, the region is characterized by centimeter-thick sandy formations that cover extensive areas (Crépy M. 2016). (Figures 3 and 4).

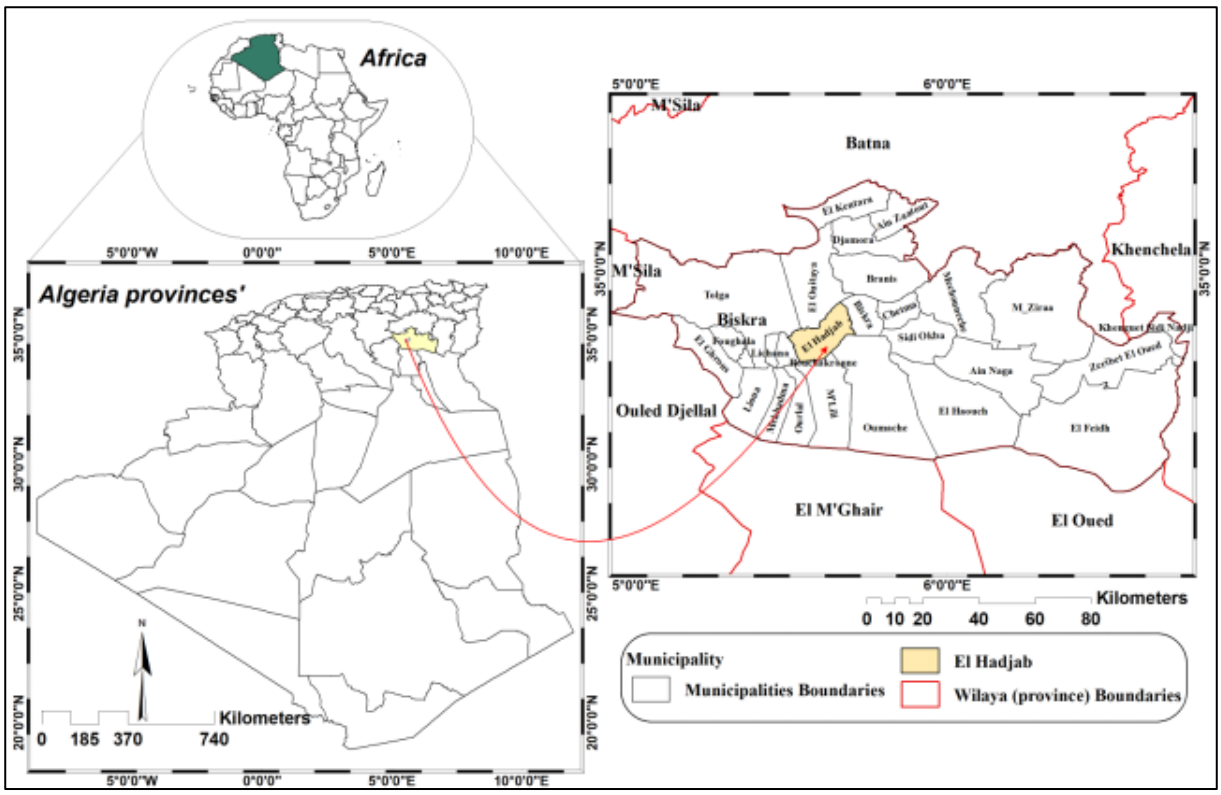

Figure 2. Area Study

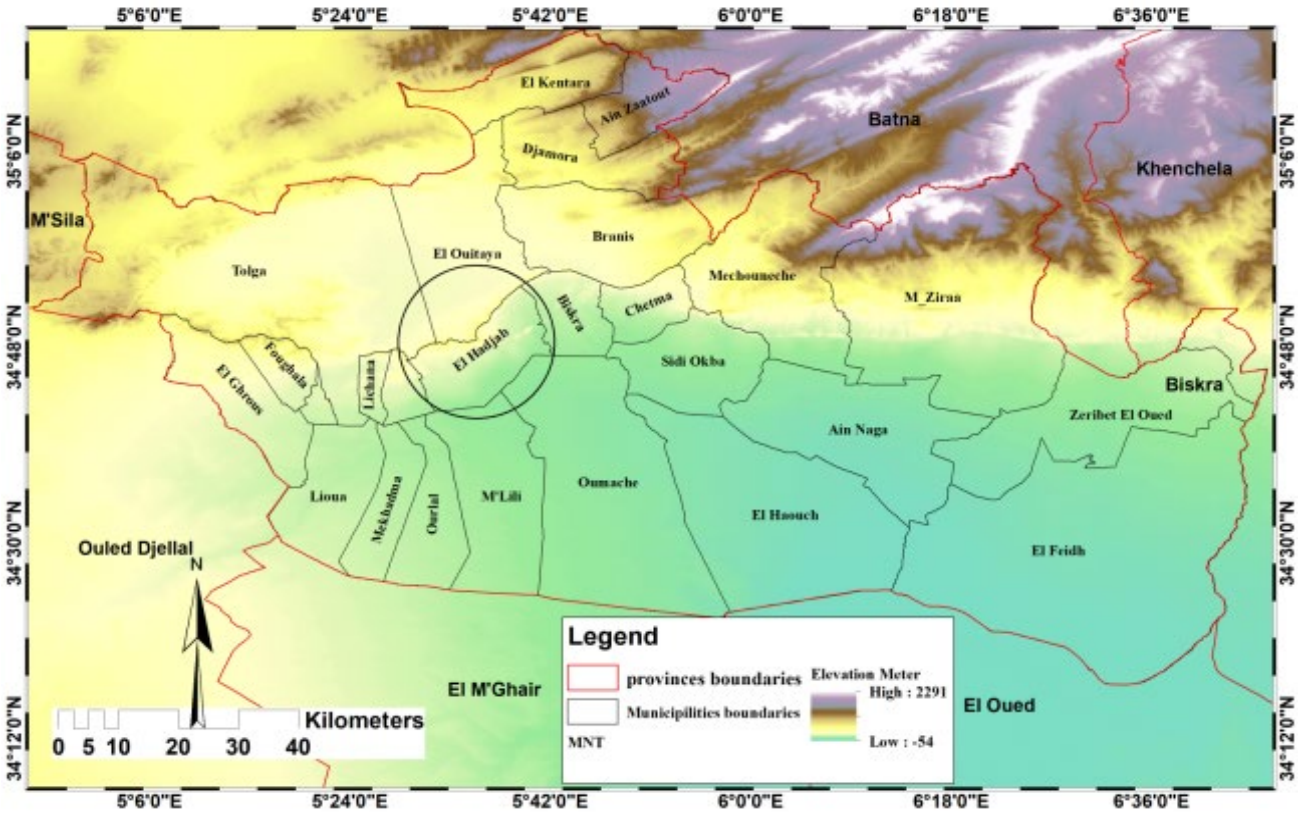

Figure 3. Topographical and geological regional features.

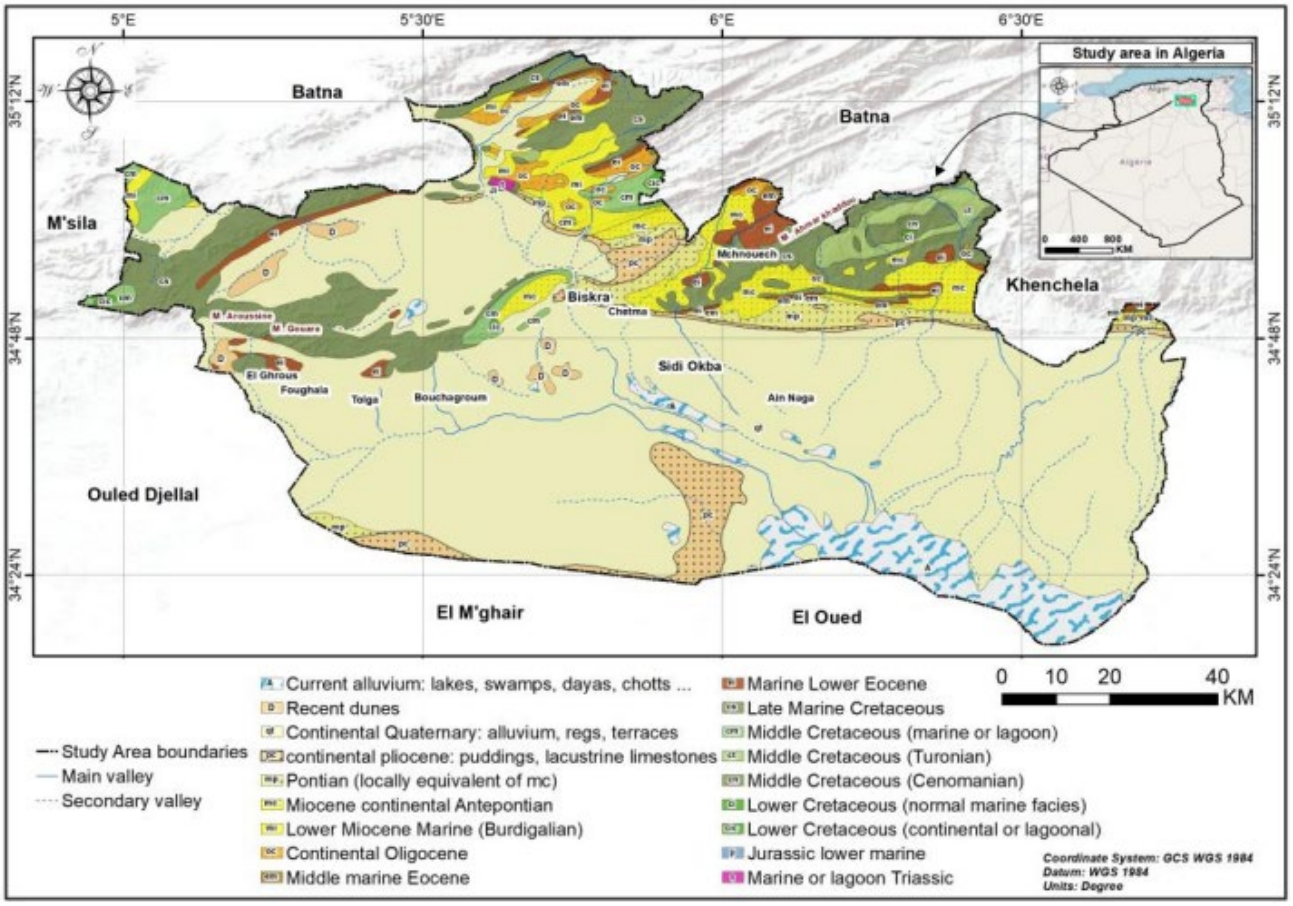

Figure 4. Geological regional features (Selahdja, 2024).

The age of these remnants is uncertain, as it could be either late Pleistocene or early Holocene. The Aeolian sands, particularly in the Ziban region, are estimated to date from approximately 7,500 to 7,000 years BP, corresponding to the arid interval at the end of the Lower Holocene (Ballais, 1993), (Figure 2).

On the southern slope of Mount Dj Bou Rhezel, at the site known as Ed Beni Brahim, the dunes cover an ablation glacis with a layer of very angular blocks that are a few decimeters thick. This layer rests on an underlying, well-sorted, fine-grained dune sand, which is devoid of coarse elements. This glacis carved into a particularly soft rock composed of an ancient dune (Ballais et al., 1979).

2.2 Climate Variability Data

2.2.1. Drought dimension:

The meteorological data utilized in this study sourced from the website (https://power.larc.nasa.gov/data-access-viewer/).

These data primarily consist of monthly rainfall series recorded at Al Hadjeb for the period 1981-2022. The data were analyzed on an annual basis to calculate the Standardized Precipitation Index (SPI).

The Standardized Precipitation Index (SPI) (Boukehlifi et al. 2025; McKee et al. 1993) is a widely recognized tool for evaluating and monitoring drought conditions. It is based on a probability distribution function of precipitation, which allows for the identification of drought events and their severity by measuring deviations from the long-term average precipitation. The SPI defined as a normalized variable.

$$\boldsymbol{SPI = (X_i - X_m)/\sigma}$$

Xi: Rainfall in year I.

Xm: Average inter-annual rainfall over the reference period.

σ: Standard deviation of inter-annual rainfall over the reference period.

The extent of a drought episode assessed by summing the indicator values for all the months during the drought period. Index values above 2.00 indicate extremely wet conditions, while values below -2.00 indicate severe drought.

Values ranging from 0.99 to -0.99 reflect conditions that are more or less normal, as outlined in Table 1 (McKee T.B. 1993). The duration covered by the SPI varies depending on the type of drought being studied and applied: for instance, the SPI will cover 1 to 2 months for a meteorological drought, 1 to 6 months for an agricultural drought, and 6 to 24 months or more for a hydrological drought. (WMO 2012).

2.2.2. Wind data

Wind data for the Al-Hadjeb region were collected over 41 years from the website the data, spanning from 1981 to 2022, include wind speeds recorded in 16 different directions. Using these data, a wind rose diagram was generated to visualize the wind patterns throughout 1981-2022. (https://power.larc.nasa.gov/data-access-viewer/).

2.2.3. Remote sensing indexes and data analysis

The Sahara Desert, with its extreme aridity and shifting dunes, faces significant challenges due to desertification. Remote sensing is crucial for monitoring these changes. By integrating spectral indices—such as BSI, MSAVI, NDVI, and NDESI—with Sentinel-1 SAR data, researchers can analyze sand movement, vegetation trends, and soil dynamics.

3. METHODS ADOPTED

This study employed a robust and integrated analytical framework designed for long-term monitoring and modeling of sand dune dynamics and land cover changes between 2004 and 2023 (Figure 1). The hybrid methodology combined multi-source remote sensing datasets, multi-decadal climate records, advanced machine learning algorithms, and geographic information system techniques to ensure temporal continuity and spatial resolution.

3.1 Acquiring and pre-processing data

Landsat 5 TM, 7 ETM+, and 8 OLI (30 m spatial resolution) were utilized to take multi-source satellite images with varying geographical, spectral, and temporal resolutions. They offered historical continuity from 2004 to 2023.

Table 1. Classification of drought according to SPI values (McKee T.B. , 1993)

SPI	**>2**	**1.50–1.99**	**1.00–1.49**	**0.50–0.99**	**−0.49–0.49**	**−0.50–−0.99**	**−1.00–−1.49**	**−1.50–−1.99**	**<−2.00**
Class	Extremely wet	Very wet	Moderately wet	Mildly wet	Normal conditions	Mild drought	Moderate drought	Severe drought	Extreme drought

Table 2. Remote sensing indexes and data analysis

Index	purposes	Data sources and period	Processes and analysis	Equation
NDESI (Normalized Difference Enhanced Sand Index)	Assess sand cover dynamics; high = active, low = stable	MODIS (2004–2023), Sentinel-1 SAR VV (2015–2023)	Preprocessing, speckle reduction, annual mean, threshold mapping	NDESI = (Red - Swir2)/(Red + Swir2) The total sand volume V (m^3) D (m): $V=A* D$ $A=\sum_{i=1}^{n}$ xi V over time t expresses as: $Vt = \int i(t)$ (https://scihub.copernicus.eu/); (Torres, R., et al., 2012); (Huang, J., et al. 2015) ; (Gagnon, A., et al. 2004).
NDVI **(Normalized Difference Vegetation Index)**	Vegetation he	Landsat / MODIS (2000–2022)	Radiometric correction, cloud masking, temporal aggregation	NDVI $=\frac{NIR+RED}{NIR+RED}$ (Bensefia, et al., 2024)
MSAVI **(Modified Soil Adjusted vgetation Index)**	Improve vege	Landsat / MODIS (2000–2022)	Radiometric correction, cloud masking, annual/seasonal aggregation	$MSAVI=\frac{2*NIR+1\sqrt{2.(NIR+1)^2-8*(NIR}}{2}$ (Qi et al., 1994 ; Broxton et al., 2014)
BSI **(Bare Soil Index)**	Quantify soil	Landsat / Sentinel (2000–2022)	Cloud masking, atmospheric correction, seasonal composites	$SBI=\frac{SWIR1+ RED-NIR-BLUE}{SWIR1+ RED+NIR+BLUE}$ (Somanathan, et al., 2024; ESRI 2021)

Sentinel-1 SAR (C-band) provided all-weather radar backscatter data starting in 2015. This data is especially useful for studying how soil moisture and surface roughness change over time.

MODIS NDVI products (250 m) were added to give high-frequency time series of vegetation patterns.

Long-term climate records (1981–2022) comprising wind speed/direction, precipitation, and temperature were used to correlate dune activity with climatic drivers.

All satellite images were subjected to radiometric and geometric corrections. Dark object subtraction (DOS) was used to reduce atmospheric effects while maintaining single-pixel co-registration accuracy. To validate the data and capture small-scale geomorphological variations not apparent in satellite data, field surveys conducted between 2019 and 2023 provided 450 ground-truth points.

3.2 Feature Extraction and Quantification

To characterize the land surface and its dynamics, both spectral and physical attributes were extracted:

Spectral Indices:

The bare soil index (BSI) is used to identify exposed soils, (Table 2).

Vegetation cover and stress using the Normalised Difference Vegetation Index (NDVI) and the Modified Soil Adjusted Vegetation Index (MSAVI), (Table 2).

Sand mobility was quantified using the Normalised Difference Sand Erosion Index (NDSEI), which was newly developed for this study.

SAR Backscatter: The Sentinel-1 VV and VH polarisation backscatter coefficients captured variations in surface roughness and moisture, allowing for the distinction between mobile and stabilised dunes regardless of cloud cover or illumination conditions, (Table 2).

These metrics were used to quantify annual changes in dune surface area (2004–2023) and volumetric changes (2015–2023).

3.3 Machine Learning Classification

3.3.1 Training Data and Classes

The training datasets consisted of 450 GPS-located field points, visual interpretation of high-resolution imagery (Google Earth Pro, 0.5-2 m resolution), and existing geomorphological maps. Four thematic land cover classes were identified: active sand dunes (moving sands), scattered sands, vegetated areas, and stable sand dunes. (https://code.earthengine.google.com/c2f8a0c70851e

9761ff4cad3f61a4f26), (Figure 5).

The input feature set consisted of multispectral bands (VIS, NIR, and SWIR), synthetic aperture radar (SAR) scattering, and four derived indices.

3.3.2 Training and parameterisation of models (Using GEE and Arc GIS Pro Tools)

Training samples were randomly split into 70% for model training and 30% for independent validation.

Random Forest (RF): Implemented as ee.Classifier.smileRandomForest (500), producing high robustness to noisy features and allowing extraction of variable importance, which highlighted NDSEI and SAR backscatter as the most discriminant features.

Support Vector Machine (SVM): Utilized an RBF kernel with cost=10 and gamma=0.5 (ee.Classifier.libsvm), optimized through five-fold cross-validation to handle non-linear class separability.

3.3.3 Multi-Year Mapping

Annual composites of spectral indices were generated (e.g., modis.filterDate(start,end).select('NDVI').mean()), producing a time series of 20 classified maps. This enabled trend analysis and inter-annual variability assessment of dune dynamics.

3.3.4. Model Evaluation

Classification accuracy was assessed using Overall Accuracy (OA), User's Accuracy (UA), Producer's Accuracy (PA), and the Kappa coefficient. Both RF and SVM achieved OA > 90% for recent years (2018–2023), with RF slightly outperforming SVM (Kappa=0.89 vs. 0.85). These high accuracies demonstrate the reliability of the classification outputs.

3.4 GIS-Based Spatial Analysis

Classified maps exported from GEE were integrated into ArcGIS Pro for advanced spatial and decision-support analysis:

Change Detection: Quantified spatial transitions between 2004 and 2023, revealing a net expansion of active dunes by 42 km² and a contraction of stabilized dunes by 30 km².

Hotspot Mapping: Overlays with agricultural and settlement layers identified high-risk zones of dune encroachment affecting ~15% of cultivated land in the study area.

Decision Support Integration: Results were combined with road networks, LULC maps, and administrative boundaries to prioritize mitigation strategies such as windbreak installation and dune stabilization programs.

This multi-tiered methodology enables not only high-fidelity mapping of dune dynamics but also provides.

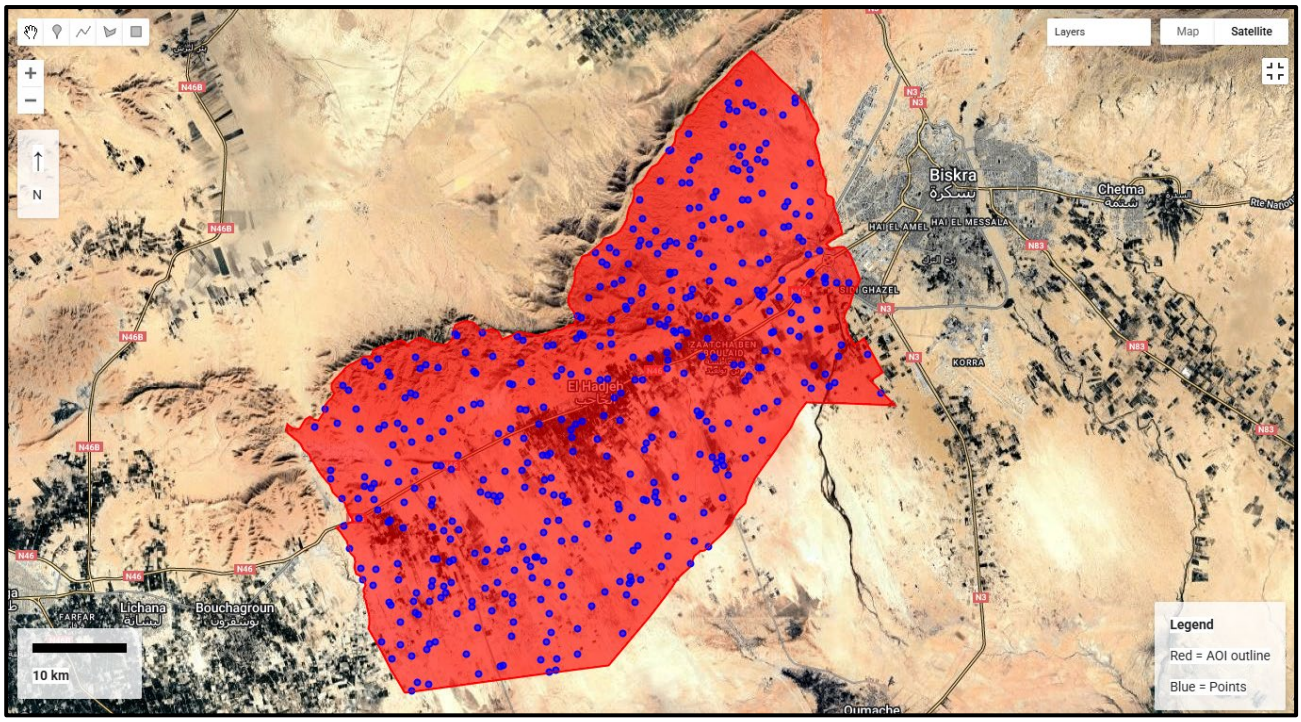

Figure 5. The training datasets of 450 locations (From Google Earth Engine)

4. RESULTS AND DISCUSSION

4.1. Sand Dune Contraction

Analysis of multi-temporal Landsat, Sentinel-1 SAR, and MODIS datasets (2004–2023), processed in Google Earth Engine (GEE) and analyzed in GIS, reveals substantial dune contraction. Classified dune area declined from 54.07% in 2004 to 42.16% in 2023, representing an 11.90% reduction in spatial extent. (Figure 6)

Machine learning classification (Random Forest) applied to spectral indices—NDVI, MSAVI, BSI, and NDSEI—combined with Sentinel-1 SAR backscatter confirmed this trend with an overall classification accuracy of 92.4% and a Kappa coefficient of 0.89. (Figure 7-8).

The heatmap generated in GEE (Figure 7) illustrates sand movement intensity, with green zones indicating stabilization, and red zones showing desertification and active dune contraction. Low SVAMI values (mean: 0.0643) suggest moisture stress, while low BSI (mean: 0.1086) indicates reduced bare soil brightness—both factors contributing to erosion vulnerability.

Bulk density measurements imply the region is at a geomorphic threshold for erosion, where soils are loose enough for aeolian transport yet compact enough to limit infiltration. (Figure 9-11)

Vegetation health declined over the study period, with mean NDVI dropping from -0.1823 to -0.2001. (Figure 10)

This aligns with desertification theory, where reduced vegetation cover destabilizes dune systems (Tucker, 1979; Schlesinger et al., 1990).

Interestingly, pixel reflectance values increased from -48.87 to -41.82, possibly indicating the presence of more resilient vegetation species or subtle changes in soil reflectance (Table 3).

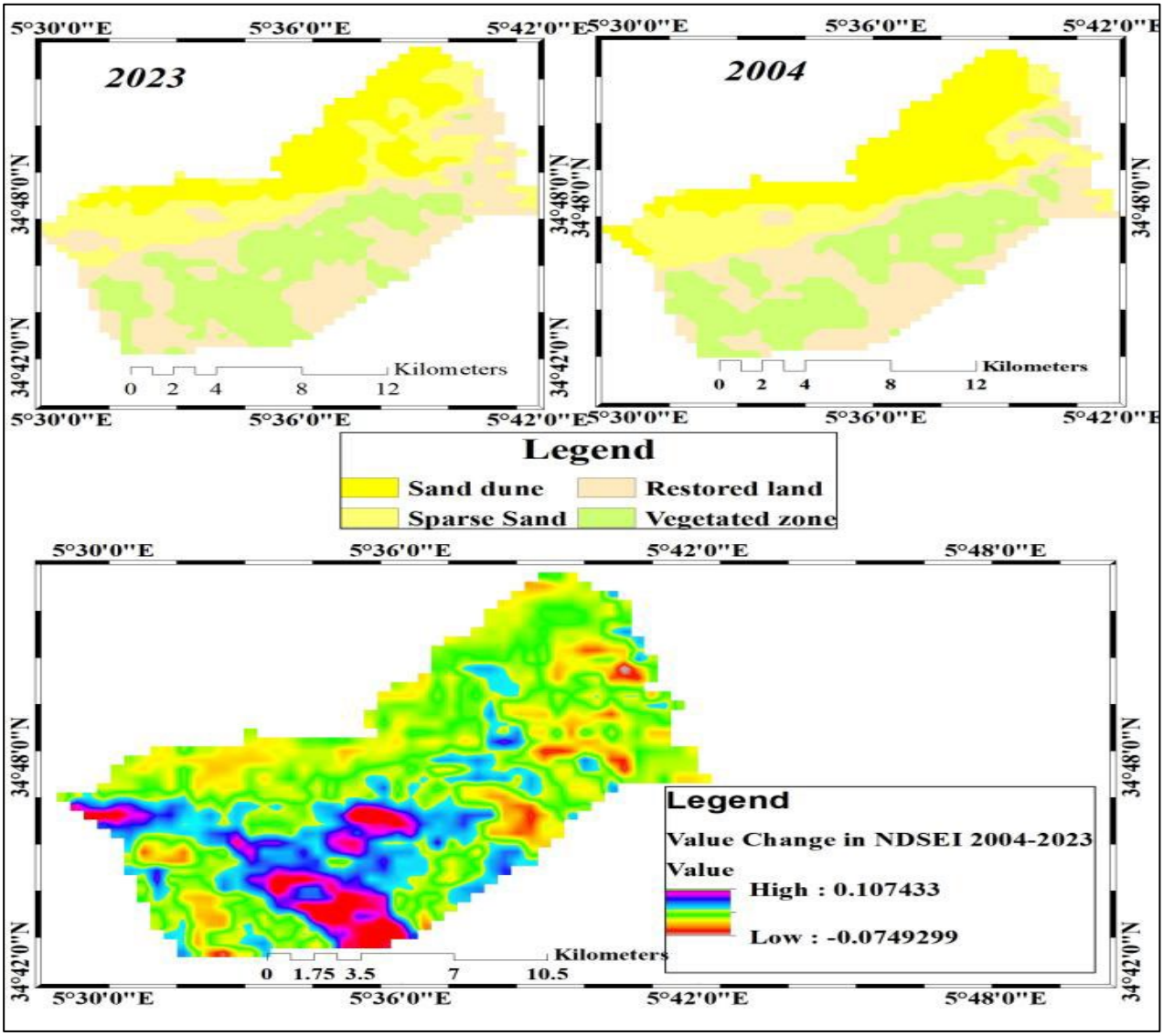

Figure 6. Land Use Land Cover shifts from 2004 to 2023.

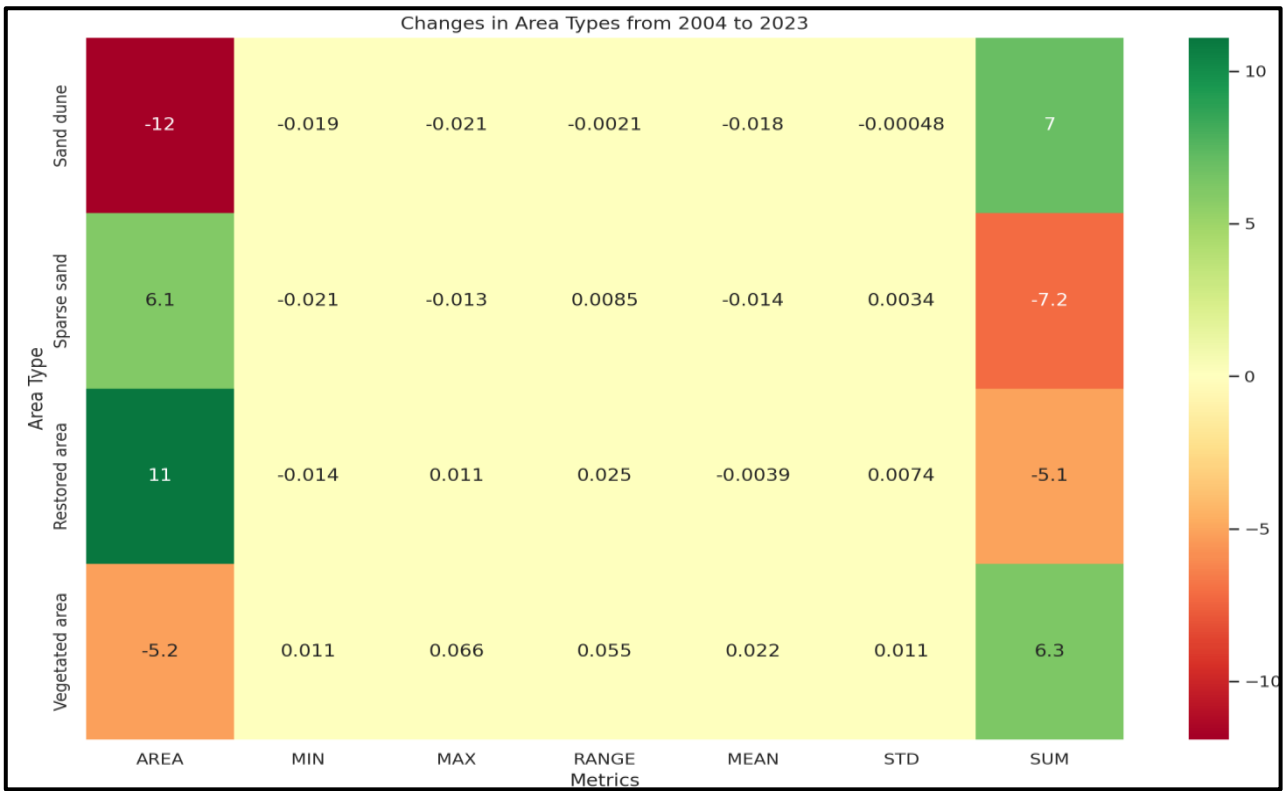

Figure 7. Heat map illustrate changes Types areas from 2004 to 2023.

Sand dune: AREA = -12 → Overall, sand dune area decreased by 12 units. SUM = 7 → Despite the overall decrease, some years had positive increases.

Sparse sand:AREA = +6.1 → Increased overall. SUM = -7.2 → But across the years, total cumulative yearly changes were negative.

Vegetated area: AREA = -5.2 → Lost some vegetation. SUM = +6.3 → But total positive changes over the years slightly outweighed losses in some periods

Table 3. Data on agricultural investment areas in the Hajeb region.

Year	Agricultural area used (Ha)	Number of palm trees	Cereals (Ha)	Open-field agriculture (Ha)	Greenhouses Number
1987	/	/	/	/	/
1998	/	116739	/	/	
2008	5484	237190	25	50	135
2018	5394	239645	9	200	103
2022	5394	240245	8	150	50.00

Source: Agriculture département of Biskra 2023.

However, the machine learning feature importance ranking placed NDSEI and BSI as stronger predictors of dune activity than NDVI, indicating that soil exposure plays a dominant role in current dune dynamics.

The increasing pixel value also hints at changes in soil moisture, as suggested by the low SVAMI values, which indicate moisture stress and its influence on vegetation growth.

4.2 Expansion of Sparse Sand Areas

The sparse sand class expanded from 36.11% in 2004 to 42.16% in 2023, marking a 6.05% increase. RF and SVM classification outputs, supported by NDVI trends becoming more negative (-0.1411 to -0.1553), confirmed this expansion is associated with higher sand content and degraded vegetation cover. Low SVAMI values corroborate increasing moisture stress, a primary factor in reduced plant establishment.

Variability within sparse sand areas increased, as shown by a broader NDVI–BSI range in 2023. The sum of pixel values for sparse sand rose from -25.25 to -32.44, indicating both areal expansion and increased surface reflectivity due to vegetation loss. Feature importance analysis from the RF model ranked SAR backscatter (VV) and BSI as critical predictors for detecting sparse sand transitions, reflecting their sensitivity to soil surface roughness and exposure.

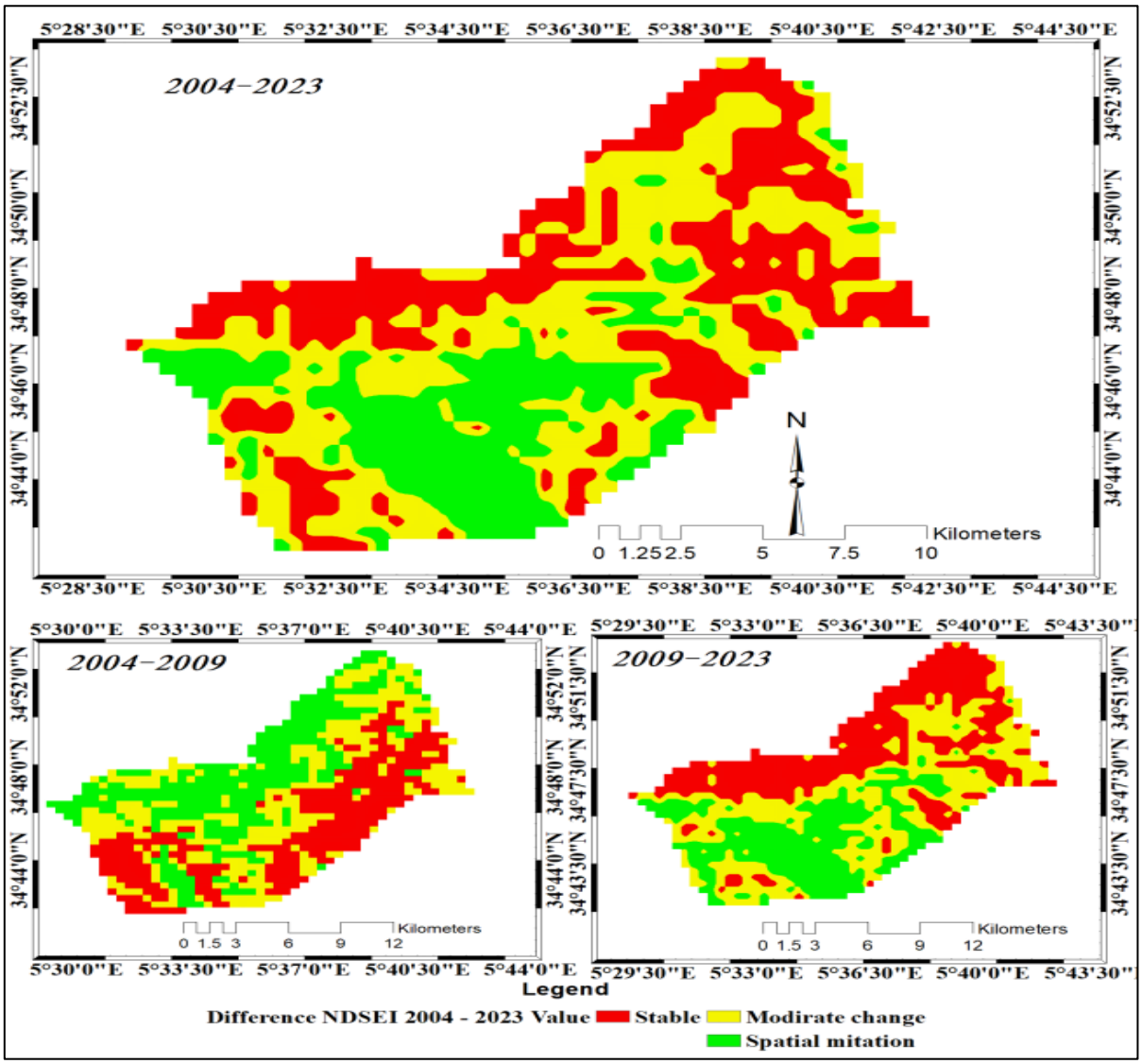

Figure 8. NDSEI spatial changes between 2004-2023.

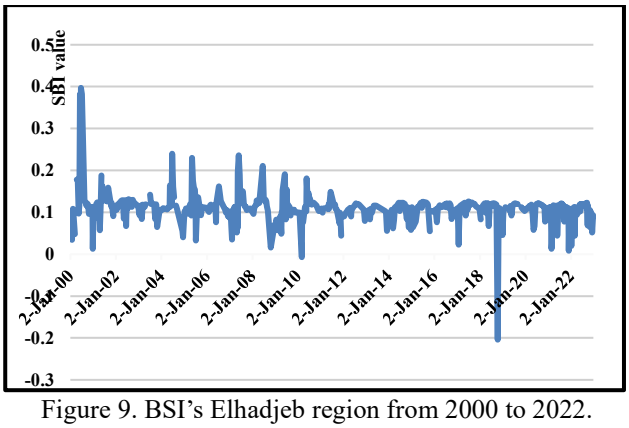

Figure 9. BSI's Elhadjeb region from 2000 to 2022.

4.3. Environmental Factors Influencing Sand Movement

Climatic drivers exert a strong influence on observed geomorphic changes. Data from the Biskra station show maximum summer temperatures reaching 40.38°C (July) and winter minima around 15.79°C (January) (Boukehlifi et al., 2025; Barroso et al., 2024). These seasonal extremes, coupled with large diurnal ranges, accelerate mechanical weathering, promoting rock disintegration into transportable sand particles (Eppes, & Keanini, 2017).

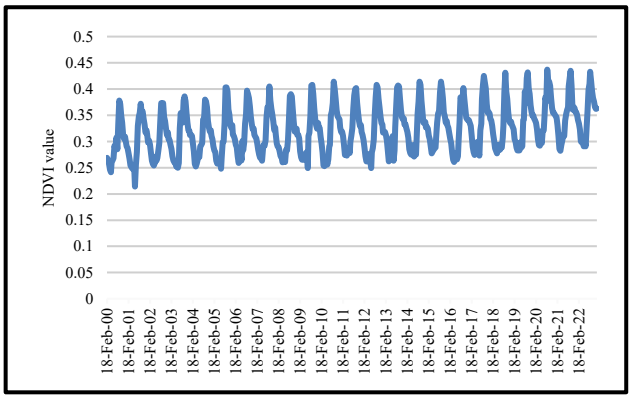

Figure 10. Vegetation surface in El Hadjeb region from 2000 to 2022 via NDVI (https://lpdaac.usgs.gov/products/mod13q1v006/).

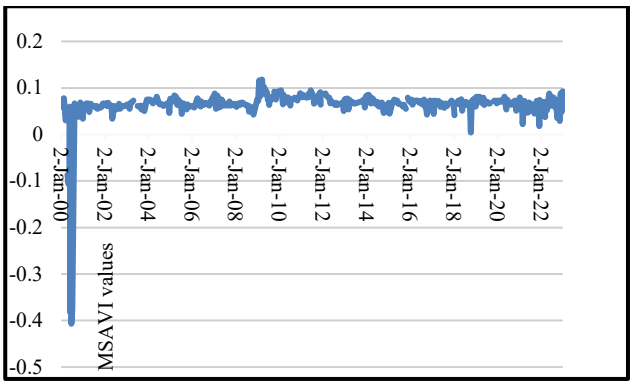

Figure 11. MSAVI's El Hadjeb region from 2000 to 2022.

The Standardized Precipitation Index (SPI) indicates a prolonged precipitation deficit from 2014–2023, exacerbating dune destabilization by reducing soil moisture, accelerating salinization, and promoting organic matter loss (Figure12).

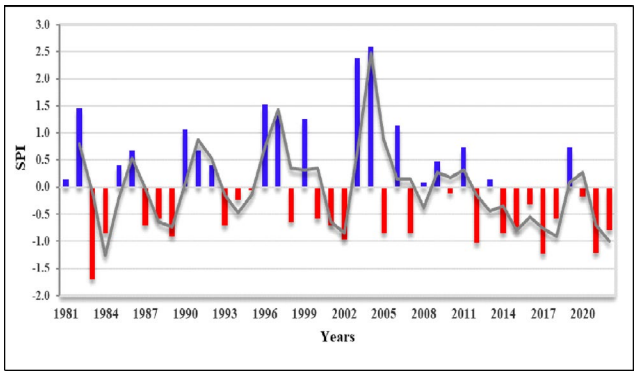

Figure 12. SPI standardized precipitation index over the period 1981-2022 El Hadjeb.

Wind patterns from the El Hadjeb station reveal dominant spring and summer high-speed winds, aligned with the observed timing of peak sand transport. GEE-based wind–sand correlation analysis showed that periods of elevated wind speed (>6 m/s) strongly aligned with SAR-detected surface roughness changes. (Figure 13).

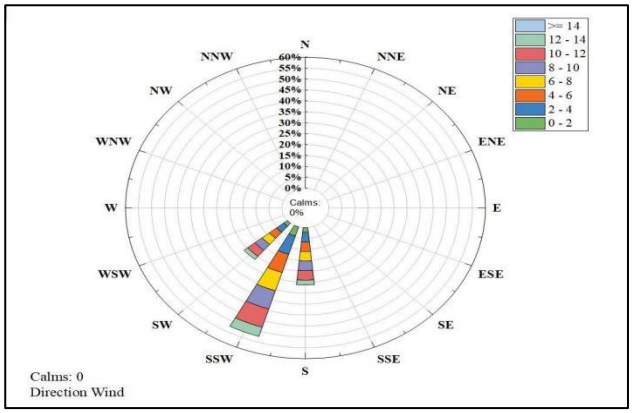

Figure 13. Wind speeds and directions in the El Hadjeb study area.

Restoration efforts, mapped using NDVI and SAR temporal composites, show localized improvements in vegetation density, which the SVM model predicts as areas of reduced sand mobility.

The observed trends emphasize the importance of restoration efforts in mitigating desertification. The expansion of sparse sand areas, alongside the growth of restored areas, suggests that restoration may be influencing sand movement dynamics. Restoration plays a crucial role in stabilizing the landscape, improving soil moisture retention, and supporting vegetation growth, which can help curb barren land spread and the growth of sparse sand areas. However, ongoing monitoring is necessary to assess the success of these efforts and refine strategies.

In conclusion, integrating NDVI, SVAMI, and SBI data with sand movement trends, alongside analysis of temperature, precipitation, and wind patterns, offers a comprehensive view of the complex interactions between vegetation health, soil moisture, and sand dynamics. The decline of sand dunes and expansion of sparse sand areas highlight the need for further research on the environmental drivers behind these changes. These findings stress the significance of addressing desertification while promoting restoration efforts. By utilizing indices like NDVI, SVAMI, and SBI, combined with climate data, we gain valuable insights, and continued research is vital to develop targeted strategies to combat desertification and support sustainable land practices.

5. CONCLUSIONS

The present study provides a comprehensive investigation into sand encroachment dynamics in El Hajeb, Algeria, from 2000 to 2023, revealing significant changes in the region's sand landscapes.

The results show an 11.90% reduction in dune areas and a 6.05% increase in sparse sand regions, largely driven by vegetation loss, soil moisture stress, and climatic factors such as prolonged droughts, high wind speeds, and rising temperatures (IPCC, 2021).

These processes contribute to desertification, as indicated by decreasing NDVI and MSAVI values (Tucker, 1979; Qi et al., 1994), which reflect vegetation stress and absence, and trends pointing to reduced soil moisture stability.

By integrating remote sensing indices—NDESI, NDVI, MSAVI, and BSI (Rondeaux et al., 1996; Xu, 2008)—with machine learning models like Random Forest and Support Vector Machines (Breiman, 2001; Cortes & Vapnik, 1995), the study produced highly accurate maps identifying critical hotspots for sand encroachment and desertification. Sentinel-1 SAR data (ESA, 2017) and Google Earth

Engine (Gorelick et al., 2017) enabled precise temporal analysis of sand cover changes, vegetation dynamics, and soil conditions. These findings highlight the vulnerability of the region's ecosystem and emphasize the growing risks to agricultural productivity, ecosystem stability, and socio-economic resources.

To mitigate desertification and stabilize the landscape, the study recommends a multi-faceted approach:

Windbreaks and Sand Fences: Establish physical barriers to reduce sand mobility and curb wind-induced erosion (Fryrear, 1985).

Afforestation and Vegetative Stabilization: Implement large-scale tree planting and restore native vegetation to enhance soil stability, improve moisture retention, and create natural barriers against sand encroachment (FAO, 2013).

Soil Management Techniques: Use organic amendments and water conservation practices to restore soil health and improve its capacity to support vegetation (Lal, 2004).

Integrated Monitoring Systems: Develop continuous monitoring frameworks combining remote sensing data with ground-based observations and socio-economic indicators to track desertification and assess intervention outcomes (UNEP, 2020).

Community Engagement: Involve local communities in restoration efforts, emphasizing awareness, training, and co-management for sustainable practices (Reij et al., 2009).

These strategies, aligned with long-term adaptive climate measures, will enhance resilience, support fragile ecosystems, and foster sustainable land management in arid and semi-arid regions.

REFERENCES

Ballais, J.-L., 1993. *Formations éoliennes et phases arides quaternaires dans le Bas-Sahara algéro-tunisien,* Würzburger Geographische Arbeiten, 87, 107.

Ballais, J.-L., Marre, A. & Rognon, P., 1979. *Périodes arides du Quaternaire récent et déplacement des sables éoliens dans les Zibans (Algérie),* Revue de Géologie Dynamique et de Géographie Physique, 21, 97.

Barroso, A.G., Michel, G.P., Zanandrea, F., Soares, M.V.A., Almeida, G.F.S., Cataldi, M., et al., 2024. *Standard Precipitation Index (SPI) applied to Socioeconomic Pathway Scenarios (SSPs) as a tool to map the distribution of droughts and potential fire hazard areas in Brazil in the face of climate change*, Copernicus Meetings. https://doi.org/10.5194/egusphere-egu24-3221.

Benazzouz, M., 1994. *Étude des interactions relief-migrations éoliennes de sable dans la région de M'Doukal (Algérie),* https://doi.org/10.3406/medit.1994.2858.

Bensaïd, A., 2006. *SIG et Télédétection pour l'étude de l'ensablement dans une Zone Aride: le cas de la Wilaya de Naâma (Algérie),* PhD thesis, Université Joseph-Fourier - Grenoble I.

Bensefia, S., Khoudour, D. J., Belayadi, A., & Lounis, S. 2024. *The status of artificial wetland areas in light of climate change using geospatial systems: Case study Ain Zada Lake (Algeria),* Geografie, 129(3), 233–263. https://doi.org/10.37040/geografie.2024.013.

Boulghobra, N., Hadri, T., & Bouhana, M., 2014. *Using Landsat imagery for monitoring the spatiotemporal evolution of sanding in dryland, the case of In-Salah in the Tidikelt (southern Algerian Sahara),* Geographia Technica, 9(1), 1-9.

Boukehlifi K. D., Athmani, H., & Bensefia, S., 2025. *Reuse of agricultural drainage water and wastewater for crop irrigation in southeastern Algeria,* Open Geosciences, 17(11). https://doi.org/10.1515/geo-2022-0749

Breiman, L., 2001. *Random forests*, Machine Learning, 45(1), 5–32. https://doi.org/10.1023/A:1010933404324.

Broxton, P. D., Zeng, X., & Sulla-Menashe, D., 2014. *The Soil Vegetation Moisture Index (SVMI) as a tool for monitoring vegetation moisture stress,* Journal of Hydrometeorology, 15(2), 603–618. https://doi.org/10.1175/JHM-D-13-0137.1

Cortes, C. & Vapnik, V., 1995. *Support-vector networks. Machine Learning*, 20(3), 273–297. https://doi.org/10.1007/BF00994018.

Cullen, K. A., 2023. *A review of applications of remote sensing for drought studies in the Andes region*, Journal of Hydrology: Regional Studies, 49, 101483. https://doi.org/10.1016/j.ejrh.2023.101483

Crépy, M., 2016. *Les Paysages du vent : géohistoire et géoarchéologie de la dépression de Kharga (désert Libyque, Égypte) du cinquième siècle avant notre ère à nos jours : 2 500 ans d'interactions entre dynamiques éoliennes et activités humaines dans un milieu hyperaride*, Doctoral thesis, Lyon.

ESA, 2017. European Space Agency. Sentinel-1 SAR User Guide. Available at: https://sentinel.esa.int/web/sentinel/user-guides/sentinel-1-sar.

Eppes, M.-C., & Keanini, R., 2017. *Mechanical weathering and rock erosion by climate-dependent subcritical cracking*, *Reviews of Geophysics, 55*(2). https://doi.org/10.1002/2017RG000557

Esri, 2021. *Bare Soil Index (BSI) Overview*, Consulted on 2024. https://www.esri.com/en-us/arcgis.

FAO, 2013. *Food and Agriculture Organization. Forest and Landscape Restoration Mechanisms*, Available at: https://www.fao.org/forestry/restoration/en/.

Fryrear, D.W., 1985. *Soil cover and wind erosion*, Transactions of the ASAE, 28(3), 781–784. https://doi.org/10.13031/2013.32321.

Gagnon, A. S., Allard, M., & Sladen, W. E., 2004. *Monitoring sand dune movement using remote sensing*, Journal of Coastal Research, 20(4), 1155–

1166.

Gorelick, N., Hancher, M., Dixon, M., Ilyushchenko, S., Thau, D. & Moore, R., 2017. Google Earth Engine: Planetary-scale geospatial analysis for everyone. Remote Sensing of Environment, 202, 18–27. https://doi.org/10.1016/j.rse.2017.06.031.

Graw, V., Bernhofer, C., Bruemmer, C., Burkhard, B., Calera, A., Dewitte, O., García, M., Menz, G., Naumann, G., Roudier, P., Rossi, S., Schmidt, M., Stoof-Leichsenring, K., & Wietler, K., 2019. *Assessment, monitoring, and early warning of droughts: The potential for satellite remote sensing and beyond*, Current Directions in Water Scarcity Research, 2, 115–131. https://doi.org/10.1016/B978-0-12-814820-4.00009-2.

Huang, J., Chen, X., Wu, J., Lu, Q., & Li, J.,2015. *Mapping sand dunes and estimating volume using remote sensing and GIS.* Geocarto International, 30(8), 891–906.

IPCC, 2021. Intergovernmental Panel on Climate Change. Sixth Assessment Report: The Physical Science Basis. Cambridge University Press. https://www.ipcc.ch/report/ar6/wg1/.

Jain, S.K. & Singh, V.P., 2003. *Water Resources Systems Planning and Management (Vol. 51, pp. 300–315). Elsevier. https://www.elsevier.com/books/water-resources-systems-planning-and-management/jain/978-0-444-51429-5.*

Kasbadji Merzouk, N., 1999. *La désertification en Algérie: Aspects climatiques, hydrologiques et pédologiques,* Thèse de Doctorat d'État, Université des Sciences et de la Technologie Houari Boumediene (USTHB), Alger, 267 p.

Lal, R., 2004. Soil carbon sequestration impacts on global climate change and food security. Science, 304 (5677), 1623–1627. https://doi.org/10.1126/science.1097396.

Manière, R., & Chamignon, C., 1986. *Cartographie de l'occupation des terres en zone aride méditerranéenne par télédétection spatiale : exemple d'application sur les Hauts-Plateaux sud oranais*: Méchéria au 1/200 000, Ecologia Mediterranea*,* 12*(1), 159–185*. https://doi.org/10.3406/ecmed.1986.1123

McKee, E. D. 1979. *Ancient sandstones considered to be eolian,* In A study of global sand seas *(U.S. Geol.* Surv. Prof. Paper 1052, pp. 187–238).

McKee, T. B., Doesken, N. J., & Kleist, J., 1993. *The relationship of drought frequency and duration to time scales*, In Proceedings of the 8th Conference on Applied Climatology (pp. 179-184). American Meteorological Society.

Moussaoui, T., Meddour, R. & Aït Yahia, K., 2022. *Analyzing desertification in arid zones using Landsat satellite images and GIS: Case study of the Algerian steppes*, Environmental Monitoring and Assessment, 194(8), 557. https://doi.org/10.1007/s10661-022-10289-6.

Mihi, A., Tarai, N., & Chenchouni, H., 2019. Can palm date plantations and oasification be used as a proxy to fight sustainably against desertification and sand encroachment in hot drylands? Ecological Indicators, 105*, 365–375.* https://doi.org/10.1016/j.ecolind.2017.11.027

Nash, D.J. & McLaren, S.J., 2003. *Kalahari sand dunes: Nature, origin, and environmental significance*, Progress in Physical Geography, 27(4), 545–576. https://doi.org/10.1191/0309133303pp391ra.

Qi, J., Chehbouni, A., Huete, A. R., Kerr, Y. H., & Sorooshian, S., 1994. *A modified soil adjusted vegetation index*, Remote Sensing of Environment, 48(2), 119–126. https://doi.org/10.1016/0034-4257(94)90134-1

Reij, C., Tappan, G., & Smale, M., 2009. *Agroenvironmental transformation in the Sahel: Another kind of "Green Revolution."* IFPRI Discussion Paper No. 00914. Washington, D.C.: International Food Policy Research Institute (IFPRI). Retrieved from https://www.ifpri.org/publication/agroenvironmental-transformation-sahel-another-kind-green-revolution

Rondeaux, G., Steven, M., & Baret, F., 1996. *Optimization of soil-adjusted vegetation indices*, Remote Sensing of Environment, 55(2), 95–107. https://doi.org/10.1016/0034-4257(95)00186-7

Selahdja, B., 2024. *The geographical distribution of prehistoric sites in the region of Biskra*, Journal el-Baheth in Human and Social Sciences, 15(1), 135-147.

Schlesinger, W. H., Reynolds, J. F., Cunningham, G. L., Huenneke, L. F., Jarrell, W. M., Virginia, R. A., & Whitford, W. G., 1990. *Biological feedbacks in global desertification*. Science, 247(4946), 1043–1048. https://doi.org/10.1126/science.247.4946.1043.

Somanathan, S. P., Kesavan, M., Parambath, S., Muraleedharan, B. V., Sreelash, K., & Damodharan, P., 2024. *A Novel Bare Soil Index for Enhancing the Mapping of Bare Soil Area – An Indicator of Urban Expansion*, Ecological Engineering & Environmental Technology, 25(10), 167-180. https://doi.org/10.12912/27197050/191455

Torres, R., Snoeij, P., Geudtner, D., Bibby, D., Davidson, M., Attema, E., … & Potin, P., 2012. *GMES Sentinel-1 mission*, Remote Sensing of Environment, 120*, 9–24.* https://doi.org/10.1016/j.rse.2011.05.028

Tucker, C. J., 1979. *Red and photographic infrared linear combinations for monitoring vegetation.* Remote Sensing of Environment, 8(2), 127–150. https://doi.org/10.1016/0034-4257(79)90013-0

UNEP, 2020. Global Environment Outlook – GEO-6: Healthy Planet, Healthy People. Nairobi: United Nations Environment Programme. https://www.unep.org/resources/global-environment-outlook-6

WMO (World Meteorological Organization), 2012. Standardized Precipitation Index User Guide.

WMO-No. 1090, Geneva, Switzerland. Consulted on [your access date], https://library.wmo.int/doc_num.php?explnum_id=7768

Wu, H., & Wilhite, D. A., 2004. *An operational agricultural drought risk assessment model for Nebraska, USA,* Natural Hazards, 33(1), 1–21. https://doi.org/10.1023/B:NHAZ.0000034994.44357.75

Xu, H., 2008. *A new index for delineating built-up land features in satellite imagery*, International Journal of Remote Sensing, 29(14), 4269–4276. https://doi.org/10.1080/01431160802039957.

Received: 14. 02. 2025
Revised: 15. 10.2025
Accepted: 17. 10. 2025
Published online: 19. 10. 2025